

Magnesium under pressure: structure and phase transition

This article has been downloaded from IOPscience. Please scroll down to see the full text article.

2003 J. Phys.: Condens. Matter 15 7727

(<http://iopscience.iop.org/0953-8984/15/45/012>)

View [the table of contents for this issue](#), or go to the [journal homepage](#) for more

Download details:

IP Address: 171.66.16.125

The article was downloaded on 19/05/2010 at 17:43

Please note that [terms and conditions apply](#).

Magnesium under pressure: structure and phase transition

F Jona and P M Marcus

Department of Materials Science and Engineering, State University of New York, Stony Brook, NY 11794-2275, USA

Received 23 July 2003, in final form 9 October 2003

Published 31 October 2003

Online at stacks.iop.org/JPhysCM/15/7727

Abstract

The pressure-induced martensitic transition of magnesium from the ground-state hexagonal-close-packed (hcp) structure at atmospheric pressure to a body-centred-cubic (bcc) structure at hydrostatic pressures larger than about 500 kbar is studied with the full-potential, linearized, augmented-plane-wave method. At any given value of the pressure, the minimum in the Gibbs free energy G , which gives the equilibrium structure, is found from the values of G along the epitaxial Bain path. This procedure, when repeated for several pressure values, allows the determination of the pressure dependence in the equilibrium state of the free energy, the volume per atom, the lattice parameters and the axial ratio for both the hcp and the bcc structures. The transition pressure is determined by the crossing of the free energies as functions of pressure for the hcp and bcc phases. The second strain-derivative of G at equilibrium at each pressure determines the elastic constants. For the shear constants c_{44} and c_{66} of the hcp structure, the internal relaxation of the second basis atom is taken into account. The elastic constants C' and c_{44} of bcc magnesium are positive and increase with pressure.

1. Introduction

Magnesium has the hexagonal-close-packed (hcp) structure at ambient pressure: an experiment [1] found that it undergoes a martensitic transformation to a body-centred-cubic (bcc) structure under hydrostatic pressure at about 500 kbar (50 GPa). This result agrees with theoretical predictions made earlier on the basis of first-principles calculations performed at zero absolute temperature [2–4] and then extended to finite temperatures [5]. These studies use total-energy methods based on the local-density-approximation (LDA) to density-functional theory: either nonperturbative linear-muffin-tin-orbital [2, 3] or *ab initio* pseudopotential methods [4], or the perturbative generalized pseudopotential theory [2, 3, 5]. The methods based on pseudopotential theory [4, 5] calculate the pressure p from differentiation of the

energy E with respect to volume V , but evaluate $E(V)$ while keeping constant the axial ratio c/a between the two lattice parameters a and c of the hcp structure.

We present here the results of a new total-energy study of the pressure-induced transition in Mg and of the elastic constants under pressure. We use the same full-potential, linearized, augmented-plane-wave method that we used successfully in previous calculations of the epitaxial Bain path (EBP) [6], but we generalize it to the case of finite hydrostatic pressure p . We thus obtain several new results, briefly enumerated here.

- (1) We find the pressure of the phase transition in Mg from rigorous theory as the intersection of the Gibbs free energy G of each phase as a function of pressure. We determine the equilibrium functions $G(p)$ and $V(p)$ for both the hcp and the bcc phases, and the pressure at the crossing point.
- (2) We evaluate the elastic constants of hcp Mg and of bcc Mg directly as functions of pressure. For hcp Mg we also calculate the bulk modulus B and the ratio k_c/k_a of the linear compressibilities along the c and the a axes (such pressure dependences are not given in previous papers).
- (3) We find that the shear constant $c_{66}(p)$ shows an extraordinary amount of relaxation as p grows, the relaxation correction being a 60% decrease from the homogeneous strain value at 600 kbar. The relaxation is calculated by a new, simpler and more accurate procedure.

The calculation procedures adopted in this study are different from those followed in previous studies of this problem. We describe our procedures in section 2, our calculations in section 3, our results in section 4, and a discussion in section 5.

2. Procedures

Consider a crystal with tetragonal or hexagonal structure. We recall that when such a crystal is at atmospheric pressure, i.e. when the applied pressure $p = 0$, the equilibrium states are conveniently found from the EBP [6], which is a special path through tetragonal or hexagonal states that goes through *all* the equilibrium states. Each state is defined by the values of the lattice parameters a and c of the corresponding tetragonal or hexagonal structure. The calculation of the EBP at $p = 0$ is done by finding at each a the value of c that minimizes the energy E , which also means that the stress σ_3 in the direction perpendicular to the basal plane (i.e. along c) vanishes [6, 7]. Hence, E along the EBP is a function of a or c/a , and the EBP is usually and conveniently presented as a plot of the energy E versus the axial ratio c/a . At any minimum of E on the EBP the first derivative of E vanishes both along the c direction (by construction) and along the EBP, which implies [7] that *all* stresses (along c as well as in the basal plane) vanish. Thus, at $p = 0$ the possible crystalline phases (tetragonal or hexagonal) of the material are given by the minima of E with respect to both a and c .

However, if $p \neq 0$ the crystalline phases are not found at the minima of E , but are found (at zero temperature) at the minima of the free energy $G \equiv E + pV$ (E = energy/atom, V = volume/atom). The minima of G in both a and c are given by the minima of G along the EBP generalized to finite p [7]. This generalization is defined as follows.

For any given value of $p \neq 0$ one chooses a value of the a parameter, but instead of seeking the value of c that minimizes the energy E (and hence causes the stress σ_3 in the c direction to vanish), one seeks the value of c that makes σ_3 equal to $-p$. The energy E at which this value of c occurs is the value to be used in $G \equiv E + pV$. This procedure is repeated for a number of choices of the a parameter (at the same p), thus finding corresponding values of c , V , and then G . The importance of G along the generalized EBP is that the minima of G are points at which the stresses in the basal plane are also equal to $-p$, and since the stress σ_3 in

the perpendicular direction is $-p$ by construction all along the EBP, the minima give possible phases under hydrostatic pressure p [7].

The possible crystalline phases found in this way may be metastable or unstable, depending on whether the conditions for stability are satisfied or not; these conditions involve the elastic constants of the phases under scrutiny [8]. To test for stability it is therefore necessary to find the elastic constants, which are calculated from the second derivatives of G with respect to appropriately chosen strains at the minima of G , just as the elastic constants for phases at $p = 0$ were calculated from the second derivatives of E with respect to strains at the minima of E (see, e.g. [9–11]).

3. Calculations

With the procedures described above we have calculated G along the EBPs for both hcp and bcc magnesium under hydrostatic pressures ranging from 0 to 700 kbar (1 GPa = 10 kbar). The total-energy calculations were done with the WIEN97 program developed by Blaha and co-workers [12]. This program uses the full-potential, linearized, augmented-plane-wave method and can calculate total energies for a variety of crystal structures and space groups with a choice of nonrelativistic (NREL) or relativistic (RELA) calculations in either the LDA or the generalized gradient approximation (GGA). In the present work we have used predominantly the NREL-LDA procedure. The program was implemented and executed on a LINUX-based desktop PC.

For the determination of total energies we used: a large plane-wave cutoff of $RK_{\max} = 9$; a magnitude $G_{\max} = 14 \text{ bohr}^{-1}$ for the largest vector in the charge-density Fourier expansion; a criterion of 1×10^{-6} Ryd for energy convergence; 4000 k -points in the full Brillouin zone (BZ) for 240–290 k -points in the irreducible wedge of the BZ, corresponding to 900–1000 plane waves; and a muffin-tin radius $R_{\text{MT}} = 1.58 \text{ bohr}$ for the Mg atom.

We now describe some details of the calculations of the EBP for a given value of the pressure p , for either hcp or bcc Mg. We select a value of a and use WIEN97 to calculate the total energy per atom E for five values of c , which are chosen to bracket the desired value of c , which we call c_p . The desired value c_p , as mentioned above, is the one at which the stress σ_3 in the c direction equals $-p$. Since [7]

$$\sigma_3 = \frac{2}{a^2 \sin \gamma} \left(\frac{\partial E}{\partial c} \right)_a, \quad (1)$$

the desired value c_p is the one at which the slope of E

$$\left(\frac{\partial E}{\partial c} \right)_a = -\frac{a^2 \sin \gamma}{2} p, \quad (2)$$

where $\gamma = 60^\circ$ for hcp Mg and $\gamma = 90^\circ$ for bcc Mg. (Since the units of E are Rydbergs and those of c are bohrs, the units of pressure in kbar or Mbar are found from $1 \text{ Ryd bohr}^{-3} = 147.11 \text{ Mbar}$.)

Having determined five values of E for the five chosen values of c , we fit a cubic polynomial to these values, differentiate the polynomial and put the derivative equal to $-(a^2 \sin \gamma)p/2$. The solution of the quadratic equation thus obtained yields two values of c , one of which (the one at positive curvature) is the desired value c_p . The energy E that corresponds to this value is then added to the term pV (with $V = c_p a^2 \sin \gamma/2$) to find G and c_p/a for the chosen value of the pressure p .

This process is repeated as many times (for as many values of a) as is necessary to find a minimum of G for the chosen p . For both hcp and bcc Mg, we have repeated the procedure

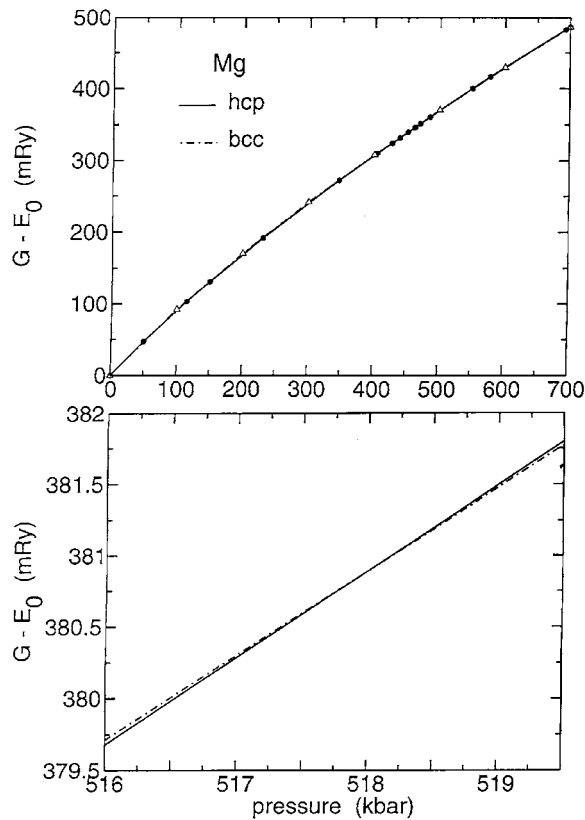


Figure 1. *Top:* free energy G versus hydrostatic pressure for hcp Mg (solid) and bcc Mg (dotted). The two curves are hardly distinguishable from one another. *Bottom:* enlarged scale, the two curves cross at about 518 kbar.

for a number of pressures between 0 and 700 kbar. We can then find the pressure dependence of G , V , a , c , and c/a for both hcp and bcc Mg at equilibrium at each p .

At each pressure p the elastic constants are calculated from second strain-derivatives of G at the minimum. The procedures are described in detail in [11] for the hcp structure and in [9, 10] for the bcc structure, both at $p = 0$. The formulae used here are the same, except that the free energy G replaces the energy E . For hcp Mg one must take into account internal relaxation, i.e. the fact that the nonequivalent atom in the hcp unit cell is free to move away from the position imposed by a homogeneous strain. Hence for hcp Mg one distinguishes between elastic constants determined with homogeneous strain, which we call *unrelaxed*, and those determined with inhomogeneous strain, which we call *relaxed*. In [11] a direct simple numerical procedure is given for calculating the relaxation effects.

4. Results

The results are presented graphically in the figures. The top panel of figure 1 is a plot of the equilibrium free energy G versus pressure p for both hcp and bcc Mg. The two curves are so close to one another that the pressure at which they cross cannot be identified precisely in this plot. We have therefore expanded the scale in the bottom panel of figure 1, which shows that the free energy of the bcc phase becomes lower than that of the hcp phase at about 518 kbar

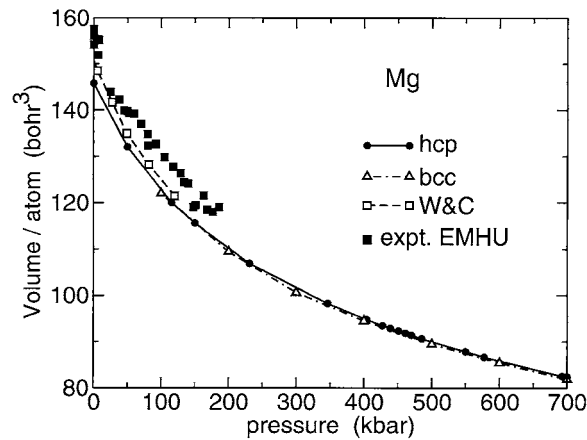


Figure 2. Atomic volumes of hcp and bcc Mg as functions of pressure. The curve between 0 and 120 kbar was calculated from the theoretical data of Wentzcovich and Cohen [4]. The solid squares are experimental data from Errandonea *et al* [13].

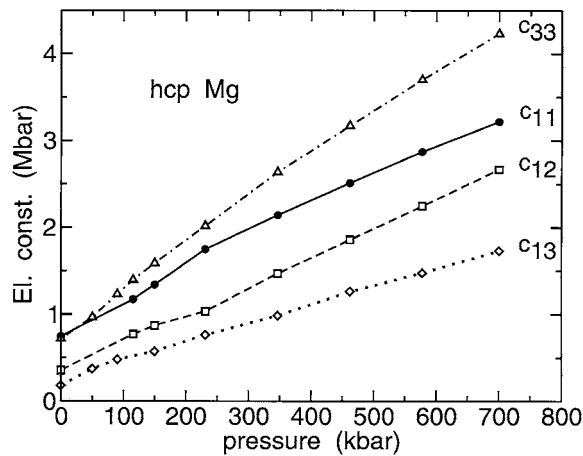


Figure 3. Pressure dependence of c_{11} , c_{12} , c_{13} , and c_{33} for hcp Mg.

and above. This result is in good agreement with experiment, which estimated the hcp–bcc transition pressure to be 500 ± 60 kbar [1].

Figure 2 shows the dependence of the volume per atom upon pressure. The curve extending from 0 to 120 kbar was calculated from the data of Wentzcovich and Cohen [4], with which the present results are in good agreement. The full squares represent results of the experimental study of Errandonea *et al* [13].

Figure 3 depicts the pressure dependence of the elastic constants c_{11} , c_{12} , c_{13} , and c_{33} for hcp Mg; figure 4 does the same for c_{44} and c_{66} , both relaxed and unrelaxed. We note that the effect of internal relaxation is very large for c_{66} : the difference between unrelaxed and relaxed values rises from about 17% at $p = 0$ to about 50–60% at higher pressures, while for c_{44} the effect is insignificant.

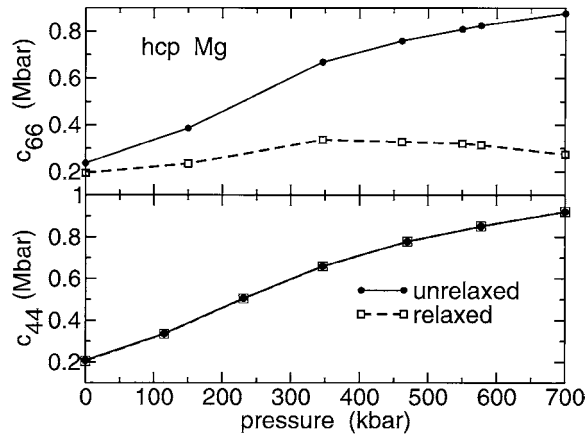


Figure 4. Pressure dependence of c_{66} and c_{44} of hcp Mg. Dashed curves: unrelaxed constants. Solid curves: relaxed constants.

From the elastic constants we have calculated the bulk modulus [14]

$$B = \frac{c_{33}(c_{11} + c_{12}) - 2c_{13}^2}{c_{11} + c_{12} + 2c_{33} - 4c_{13}} \quad (3)$$

and the ratio of linear compressibilities k_c and k_a along the c and the a axis, respectively:

$$\frac{k_c}{k_a} = \frac{c_{11} + c_{12} - 2c_{13}}{c_{33} - c_{13}}. \quad (4)$$

These two quantities are plotted against pressure in figure 5. The ratio of linear compressibilities along c and a is one measure of elastic anisotropy. We see that the anisotropy is quite large at zero pressure (about 40%) and becomes negligible at about 100 kbar and above.

For the bcc phase we have calculated two elastic constants: $C' \equiv (c_{11} - c_{12})/2$ and c_{44} . Both increase monotonically with pressure, as expected, with no anomaly at the transition.

5. Discussion

The present calculations are in good agreement with other calculations and with experiment in fixing the phase-transition pressure, which we find from the free energy of the bcc phase becoming lower than that of the hcp phase at and above hydrostatic pressures of about 518 kbar (the calculations apply to 0 K, the experiment finds the transition at 50 ± 6 GPa at room temperature [1]). This result is obtained with procedures different from those followed in previous studies of this problem, namely, from rigorous theory at the intersection of the Gibbs free energies as functions of pressure of the two phases involved.

We note that a recent experimental study of the phase behaviour of Mg in the pressure-temperature range up to 18.6 GPa and 1527 K [13] finds an hcp to dhcp transition above 9.6 GPa and high temperatures. The dhcp structure is a subtle distortion of the hcp structure: it has a stacking ABACABAC . . . , as opposed to the stacking ABABAB . . . of the hcp structure. The finding of the dhcp phase had some interesting precursors. One can be found in an early paper by Perez-Albuerne *et al* [15] which reported detecting some indications of the possible existence of a dhcp phase in Mg under pressure. The other is related to a study of the pressure dependence of the transverse-optical Γ -point mode by Olijnyk [16], who found an unusual broadening and splitting of this mode above 10 GPa. A tentative explanation for

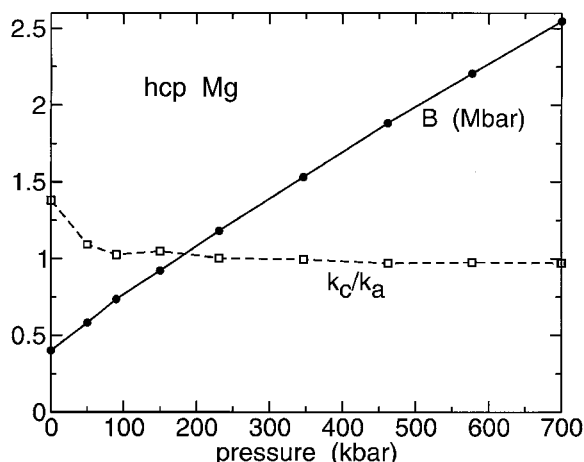


Figure 5. Pressure dependence of the bulk modulus B and of the ratio k_c/k_a between linear compressibilities k_c along the c axis and k_a along the a axis of hcp Mg.

this phenomenon was offered as due to the possible existence of a dhcp phase. The correct structure sequence of Mg as a function of pressure should therefore be hcp–dhcp–bcc. Our calculations did not consider the dhcp phase, as they were made only for hcp and bcc Mg. But total-energy calculations should find the dhcp phase to be metastable at 0 K up to 10 GPa; above 10 GPa its free energy would become lower than that of the hcp phase.

The existence of a bcc phase above 50 GPa was also confirmed indirectly by Olijnyk's study of the transverse-optical mode mentioned above [16]. In that study the Raman signals were not detected above 50 GPa: this result is consistent with the existence of a bcc structure, since this structure, with one atom per unit cell, has no optical phonon modes and therefore produces no Raman signals.

We discuss now some comparisons between our results and available experimental data. In the plot of the equation of state (figure 2) we have added the experimental data of Errandonea *et al* [13] as full squares. The trend with pressure is about the same, although the absolute values are different, but the difference between calculation and experiment is, e.g. at 150 kbar, 3.3%. Normally, in the LDA, calculated lattice parameters differ from the experimental ones by 1–2%, so that a difference in volume of 3–4% is quite understandable.

We have also calculated (but not depicted) the pressure dependence of the axial ratio c/a for both hcp and bcc Mg. Both quantities are essentially flat with pressure, although for hcp Mg the axial ratio has a negative slope in the range from 0 to about 50 kbar. This slope is calculated to be $-1.5 \times 10^{-4} \text{ kbar}^{-1}$, in good agreement with the experimental value of -1.1×10^{-4} found from the data of Errandonea *et al* [13]. The experimental data keep decreasing with increasing pressure up to 186 kbar, while our calculated data become almost flat after about 100 kbar, but at 150 kbar calculation and experiment differ only by about 0.8%.

The calculated values at zero pressure of the bulk modulus B and its pressure dependence $\delta B/\delta p$ at $p = 0$ for hcp Mg are 401 kbar and 3.6–3.8, respectively, in good agreement with the experimental results of 368 ± 30 and 4.3 ± 0.4 kbar, respectively, of Errandonea *et al* [13].

We also find the elastic constants of both hcp and bcc Mg directly as functions of pressure. For the elastic constants c_{66} and c_{44} of hcp Mg, we calculate both the unrelaxed and the relaxed values; for c_{66} we find a large relaxation which increases with increasing hydrostatic pressure. All elastic constants increase with increasing pressure, a result that is a general property of

most solids. This behaviour can be qualitatively explained by the fact that increasing pressure squeezes atoms together and hence requires stronger forces to produce a given strain.

The pressure dependence of the calculated elastic constants c_{ij} depicted in figures 3 and 4 allows us to estimate the pressure derivatives $\delta c_{ij}/\delta p$, which can be compared with available experimental data. Some such data are available from older papers: for Mg [17] up to 65 kbar, for other hcp metals, Zr [18], Ti [19], and Cd [14], only about up to about 5 kbar. We calculate the slopes of our $c_{ij}(p)$ from 0 to 150 kbar to be: $\delta c_{11}/\delta p = 3.94$; $\delta c_{12}/\delta p = 3.41$; $\delta c_{13}/\delta p = 2.60$; $\delta c_{33}/\delta p = 5.79$; $\delta c_{44}/\delta p = 1.12$; $\delta c_{66}/\delta p = 0.27$. These numbers are in fair agreement with those found experimentally for Mg and for Zr, Ti and Cd, which are, in the same order as above (— indicates that no experimental data have been found): 6.11 (Mg), 3.93 (Zr), 5.01 (Ti), 8.50 (Cd); —(Mg), 3.42 (Zr), 4.11 (Ti), 3.93 (Cd); —(Mg), 4.25 (Zr), 4.05 (Ti), 2.40 (Cd); 7.22 (Mg), 5.49 (Zr), 4.88 (Ti), 6.48 (Cd); 1.36 (Mg), -0.22 (Zr), 0.52 (Ti), 1.72 (Cd); —(Mg), 0.26 (Zr), 0.45 (Ti), 2.28 (Cd).

In summary, the present calculations show that modern first-principles electronic theory can reliably find equilibrium structures, their elastic constants, stable and metastable phases and phase transitions as functions of pressure over large pressure ranges with modest computational facilities. Among the accomplishments, we note that the calculated equation of state fits experiment well and that the sensitive measure of structural anisotropy k_c/k_a shows that isotropy is produced at 100 kbar and above. Particularly satisfying is the location of the phase transition to bcc structure above 500 kbar in agreement with experiment.

Acknowledgments

We gratefully acknowledge partial support of this work by the National Science Foundation with Grant DMR0089274.

References

- [1] Olijnyk H and Holzapfel W B 1986 *Phys. Rev. B* **31** 4682
- [2] Moriarty J A and McMahan A K 1982 *Phys. Rev. Lett.* **48** 809
- [3] McMahan A K and Moriarty J A 1983 *Phys. Rev. B* **27** 3235
- [4] Wentzcovitch R M and Cohen M L 1988 *Phys. Rev. B* **37** 5571
- [5] Althoff J D, Allen P B, Wentzcovitch R M and Moriarty J A 1993 *Phys. Rev. B* **48** 13253
- [6] Marcus P M and Alippi P 1998 *Phys. Rev. B* **57** 1971
- [7] Marcus P M, Jona F and Qiu S L 2002 *Phys. Rev. B* **66** 064111
- [8] Nye J F 1957 *Physical Properties of Crystals* (London: Oxford University Press) pp 140–2
- [9] Jona F and Marcus P M 2001 *Phys. Rev. B* **63** 094113
- [10] Jona F and Marcus P M 2002 *Phys. Rev. B* **65** 155403
- [11] Jona F and Marcus P M 2002 *Phys. Rev. B* **66** 094104
- [12] Blaha P, Schwarz K and Luitz J 1997 *WIEN97, A Full Potential Linearized Augmented Plane Wave Package for Calculating Crystal Properties* Technical University of Vienna (ISBN 3-9501031-0-4)
This is an improved and updated Unix version of the original copyrighted WIEN-code, which was published by Blaha P, Schwarz K, Sorantin P and Trickey S B 1990 *Comput. Phys. Commun.* **59** 399
- [13] Errandonea D, Meng Y, Häusermann D and Uchida T 2003 *J. Phys.: Condens. Matter* **15** 1277
- [14] Saunders G A and Yagci Y K 1986 *J. Phys. Chem. Solids* **47** 421
- [15] Perez-Albuern E A, Clendenen R L, Lynch R W and Drickamer H G 1966 *Phys. Rev.* **142** 392
- [16] Olijnyk H 1999 *J. Phys.: Condens. Matter* **15** 6589
- [17] Schmunk R E and Smith C S 1959 *J. Phys. Chem. Solids* **9** 100
- [18] Fisher E S, Manghnani M H and Sokolowski T J 1970 *J. Appl. Phys.* **41** 2991
- [19] Fisher E S and Manghnani M H 1971 *J. Phys. Chem. Solids* **32** 657